Solution combustion synthesis of Nano sized ferroelectric (1-x)$KNbO_3$-x($BaNi_{1/2}Nb_{1/2}O_{3-\delta}$): characterization, mechanism and photocatalytic properties

S. Abhinay, Ranabrata Mazumder

Department of Ceramic Engineering, National Institute of Technology, Rourkela, Odisha-769008, India

Introduction

Excessive dependence on fossil fuel

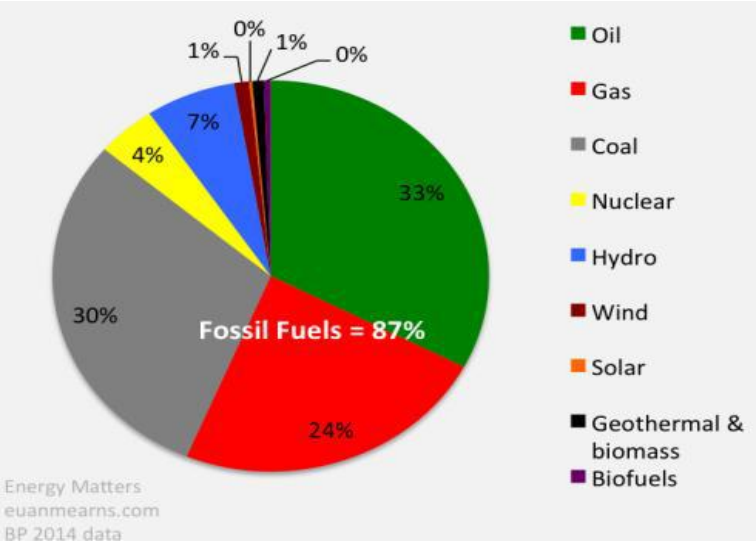

Environmental issues with toxic dyes/chemicals

Solar energy can be useful for power generation , catalytic degradation of toxic dyes and can generate clean fuel from water

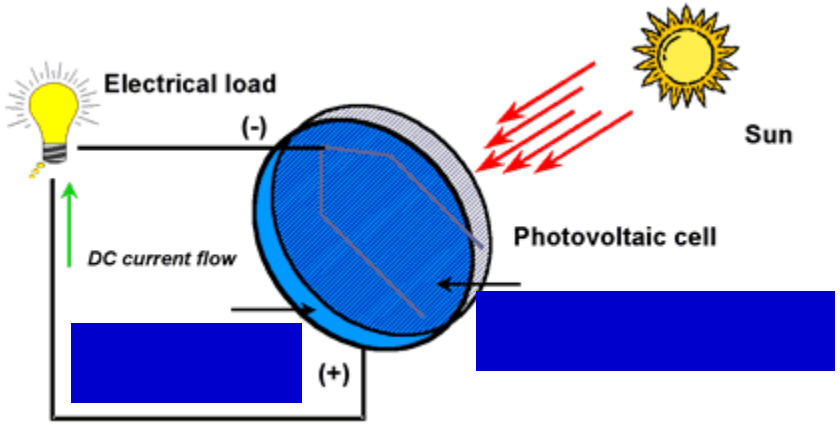

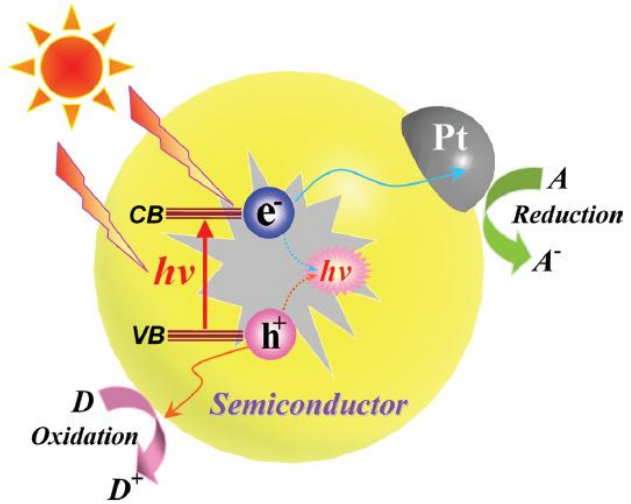

Importance of oxide ferroelectrics for photovoltaic/Photocatalytic application

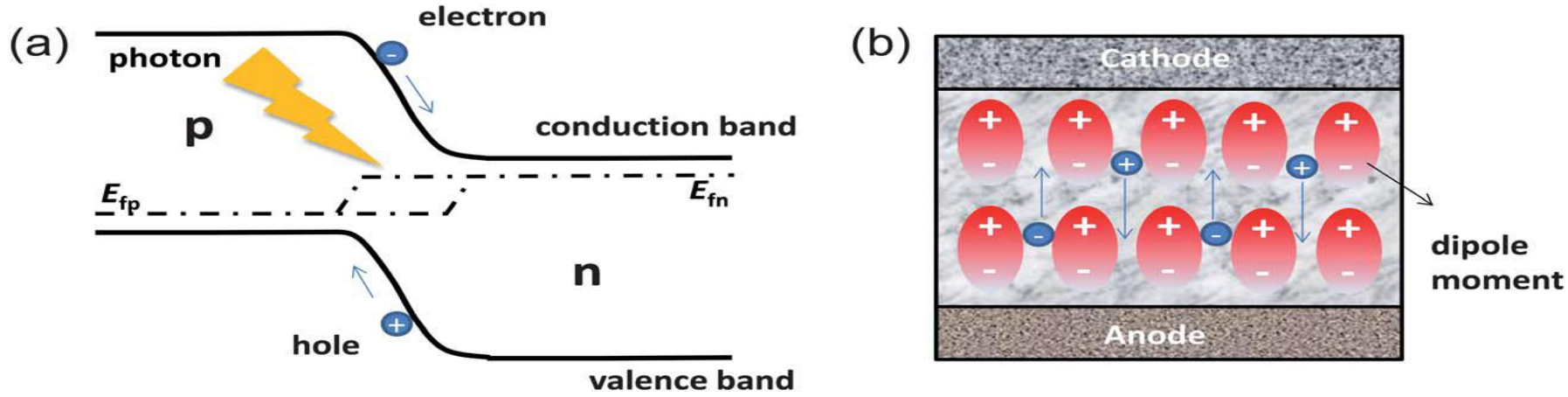

The working principle of (a) p–n junction solar cells and (b) Ferroelectric-PV devices

- **The open circuit photovoltage cannot exceed the energy barrier height of the junction, which is usually lower than 1 V.**
- **In contrast, for the ferroelectric bulk photovoltaic effect, the remnant polarization and the polarization-induced internal electric field exist over the whole bulk region of the ferroelectric rather than a thin interfacial layer. In this case, the charge transportation is not limited by diffusion, and the output photovoltage is not limited by any energy barrier.**

- C. Xu, J. Wu, U.V. Desai, Di Gao, Nano Lett., 12, 2420−2424 (2012).
- W. Wang, M. O. Tade´a and Z. Shao, Chem. Soc. Rev., 44, 5371-5408 (2015).

Conti…….

- ✓ **Photovoltaic effect in ferroelectrics is essentially a sort of bulk-based effect, which differs from the conventional junction-based interfacial photovoltaic effect in semiconductors**
- ✓ **It has been proposed that the dipole moment of a polar molecule (or induced dipole moment) interacts with the polarization of ferroelectric domains at the surface. This reduces the energy required to break bonds and enhances the photochemical activity**
- ✓ **Due to surface charges band bending occurs at the surface**

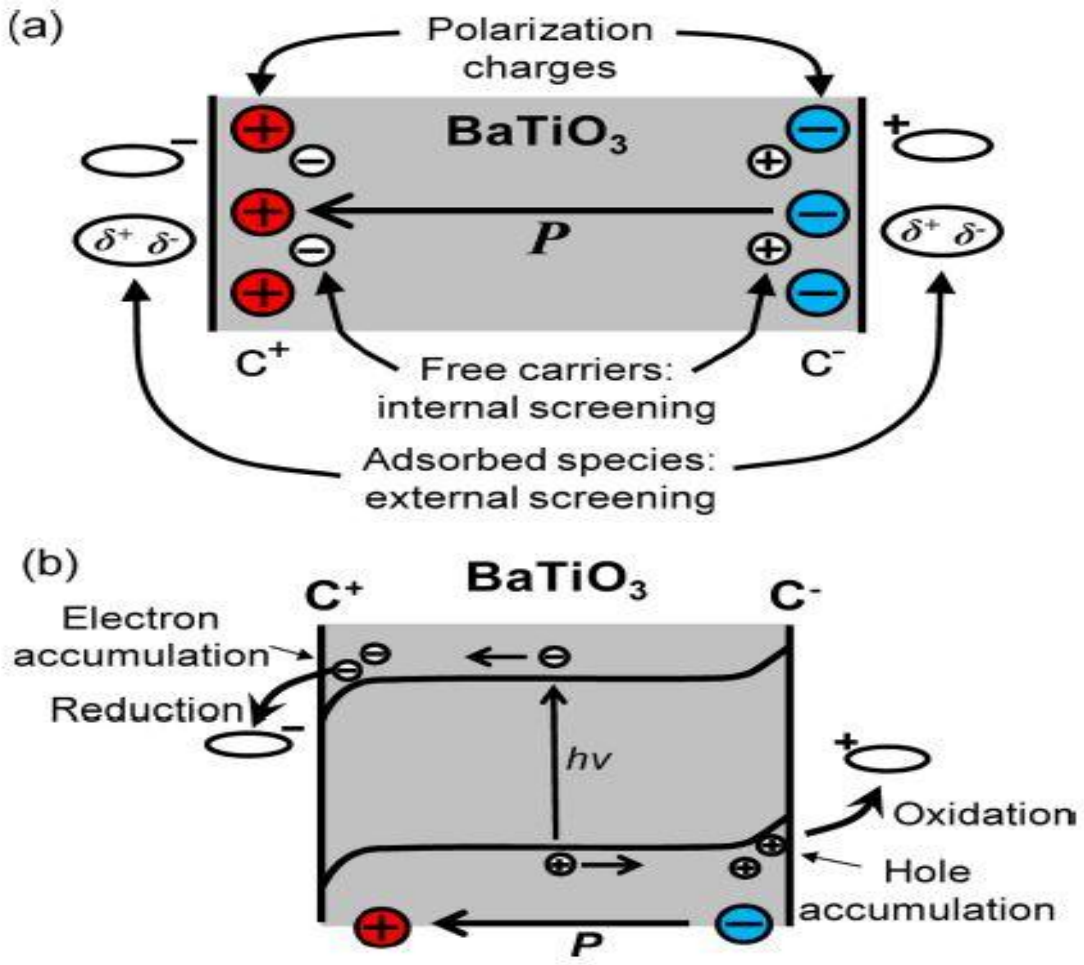

Schematic of a ferroelectric material showing (a) internal polarization and screening mechanisms and (b) the effect of free carrier reorganization on band structure and photoexcited carriers.

S. Dunn et al., Chem. Mater. 2013, 25, 4215−4223

Drawbacks of the use of conventional ferroelectric ceramics in photocatalytic/photovoltaic application?

- In most of the cases photocurrent generated from conventional ferroelectric is in the nA/cm^2 range and efficiency < 0.5%, restricts their practical use. Further improvements in photovoltaic efficiency have been inhibited by the wide bandgaps of ferroelectric oxides.

- The current ferroelectric oxides have wide band gaps (E_g>2.7 eV for $BiFeO_3$, E_g>3.5 eV for PZT) that are beyond the visible-light range and thus allow the use of only 8%–20% of the solar spectrum.
- There are need of the hour is to engineer materials which have sufficient absorption of the solar radiation (band gap below 2 eV), efficient separation of the photo-excited charge carriers (ideal is ferroelectric materials), and a low charge recombination rate.

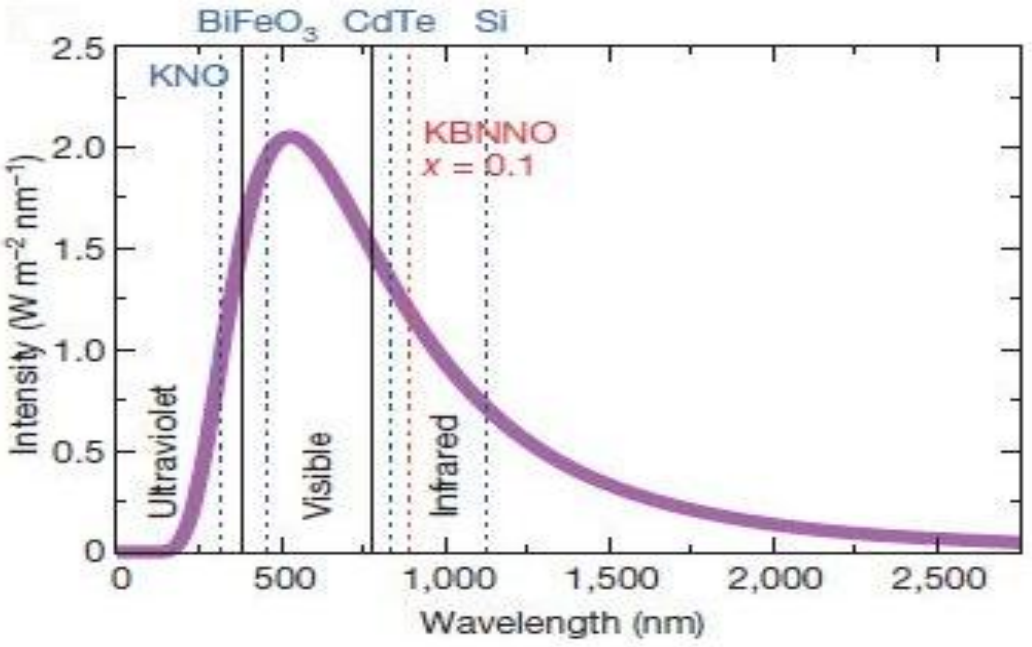

- W. Dong, Y. Guo, B. Guo, H. Li, H. Liu, Mater. Lett., 88, 140-142, (2012).
- H. Sharma, S. Bobby singh, N. Boinis singh, Phys. B., 406, 351-353, (2011).

Why Ba, Ni modified $KNbO_3$

- Bandgap < 2 eV can utilize sunlight efficiently
- Photocurrent density 50 times larger than classic ferroelectric (Pb,La)(Zr,Ti)O3
- Photo response properties measured on thick ceramic sample (20- 50 µm)
- V_{oc} ~ 3.5 V, J_{sc} ~ 0.1 µA/cm^2

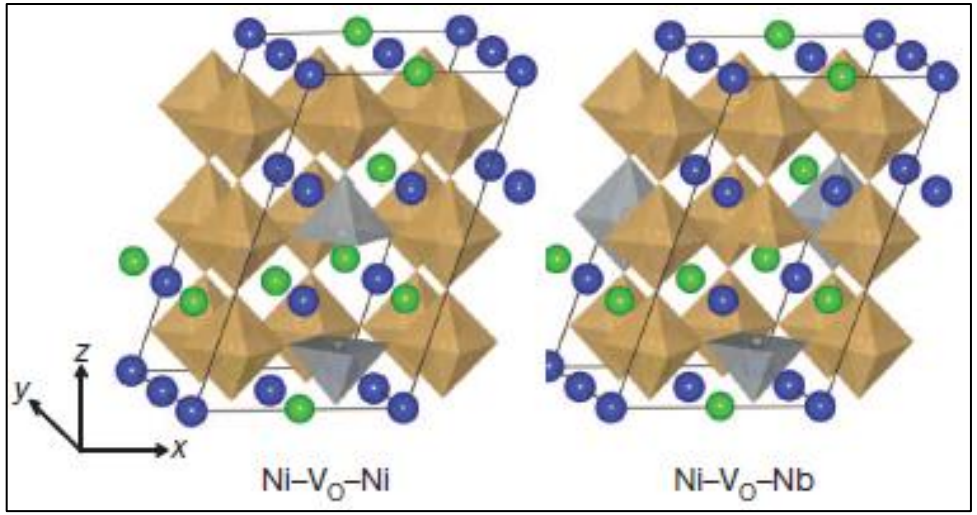

[KNbO3]1-x [Ba(Ni1/2Nb1/2)O3-δ]x crystal structures K and Ba are shown by blue and green spheres, respectively; NbO6 and NiO6 are shown as brown and grey octahedra with O atoms at the vertices.

Issues need to be addressed

- ❑ Requires high phase formation (950^{o}C/24h) and sintering temperature (1100^{o}C/6h)
- ❑ Drastic reduction in processing temperature required
- ❑ Photocatalytic property not studied and
- ❑ Effect of particle size on photocatalytic also not studied

I. Grinberg, D. V. West, M. Torres, G. Gou, D. M. Stein, L. Wu, G. Chen, E. M. Gallo, A. R. Akbashev, P. K. Davies, J. E. Spanier, A. M. Rappe, Nature 503, 509 (2013).
W.S.Choi, M. F. Chisholm, D. J. Singh, T. Choi, and G. E. Jellison, Nat. Commun. 3, 689 (2012).

OBJECTIVES

- To synthesize phase pure $(1-x)KNbO_3-x(BaNi_{1/2}Nb_{1/2}O_{3-\delta})$ (x= 0, 0.05, 0.1, 0.15, 0.2) at low temperature by using solution combustion synthesis (avoiding alkoxide precursors)

- To study the effects of fuel to oxidizer ratio on phase evolution and powder properties

- To study the photocatalytic behavior of the synthesized powder.

Solution Combustion Synthesis

- Low temperature for phase formation
- Mixing at molecular level (homogeneity is maintained)
- High purity
- Fine particle size
- Simple, fast and energetically economic
- Fuel to metal ratio (G/M), fuel to oxidizing agent (F/O), temperature and sometimes pH of the solution, can be varied to get desired morphology of powder.

Process parameters influencing Solution Combustion Synthesis
▪ Fuel to Oxidizer ratio
▪ Metal to fuel/ Complextant ratio
▪ Precursor concentration
▪ pH of the Solution

Role of in ϕe Combustion synthesis

$$\phi_e = \frac{\sum(coefficients\ of\ oxidising\ elements\ in\ the\ spefic\ formula \times oxidising\ valence)}{(-)\sum(coefficients\ of\ reducing\ elements\ in\ the\ specific\ formula\ \times reducing\ valence)} = p/r$$

Experimental procedure

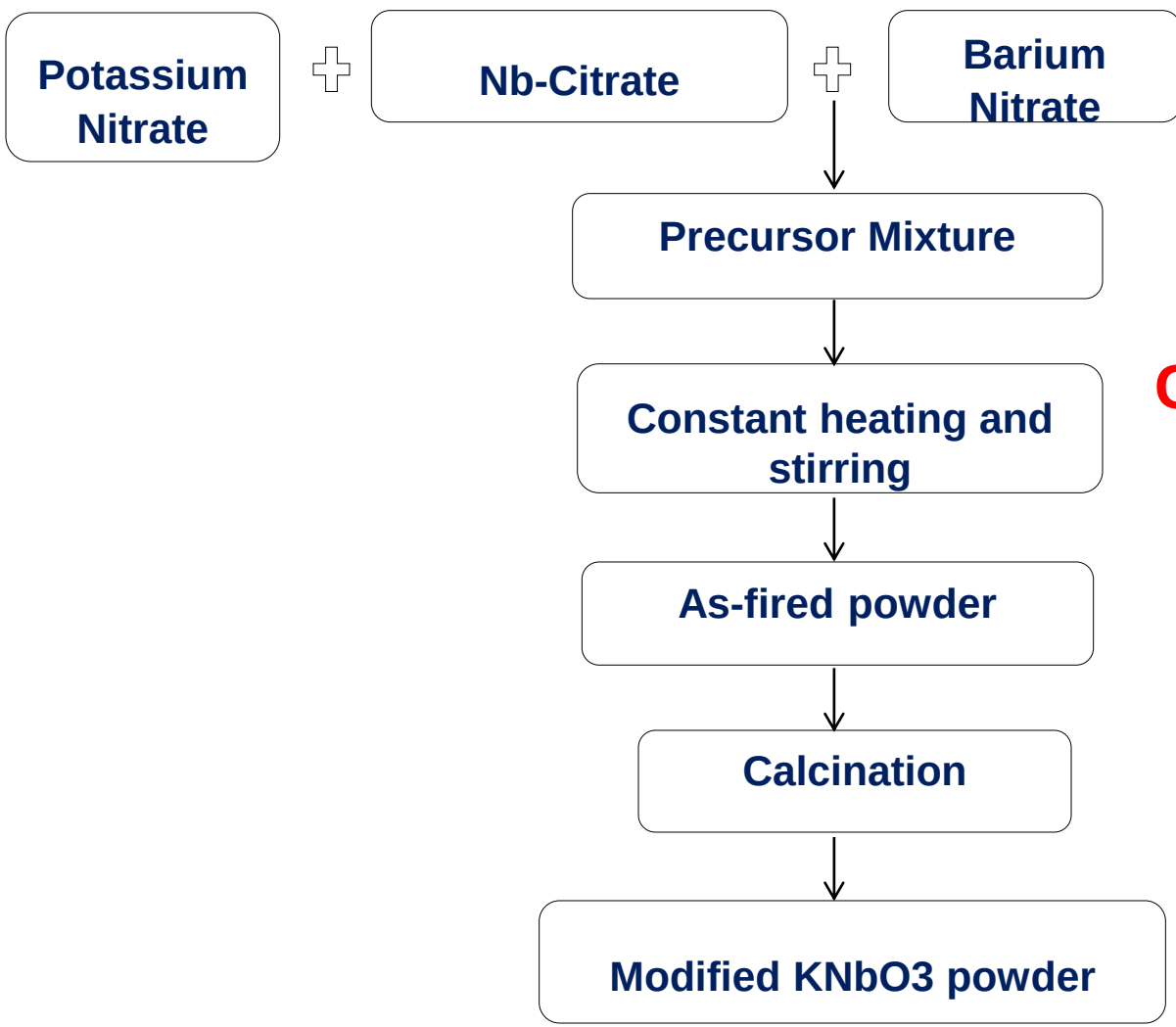

Characterizations

- FTIR and XRD of gel/powder samples
- Raman spectroscopy
- XPS
- TEM
- Optical properties

Results & Discussion

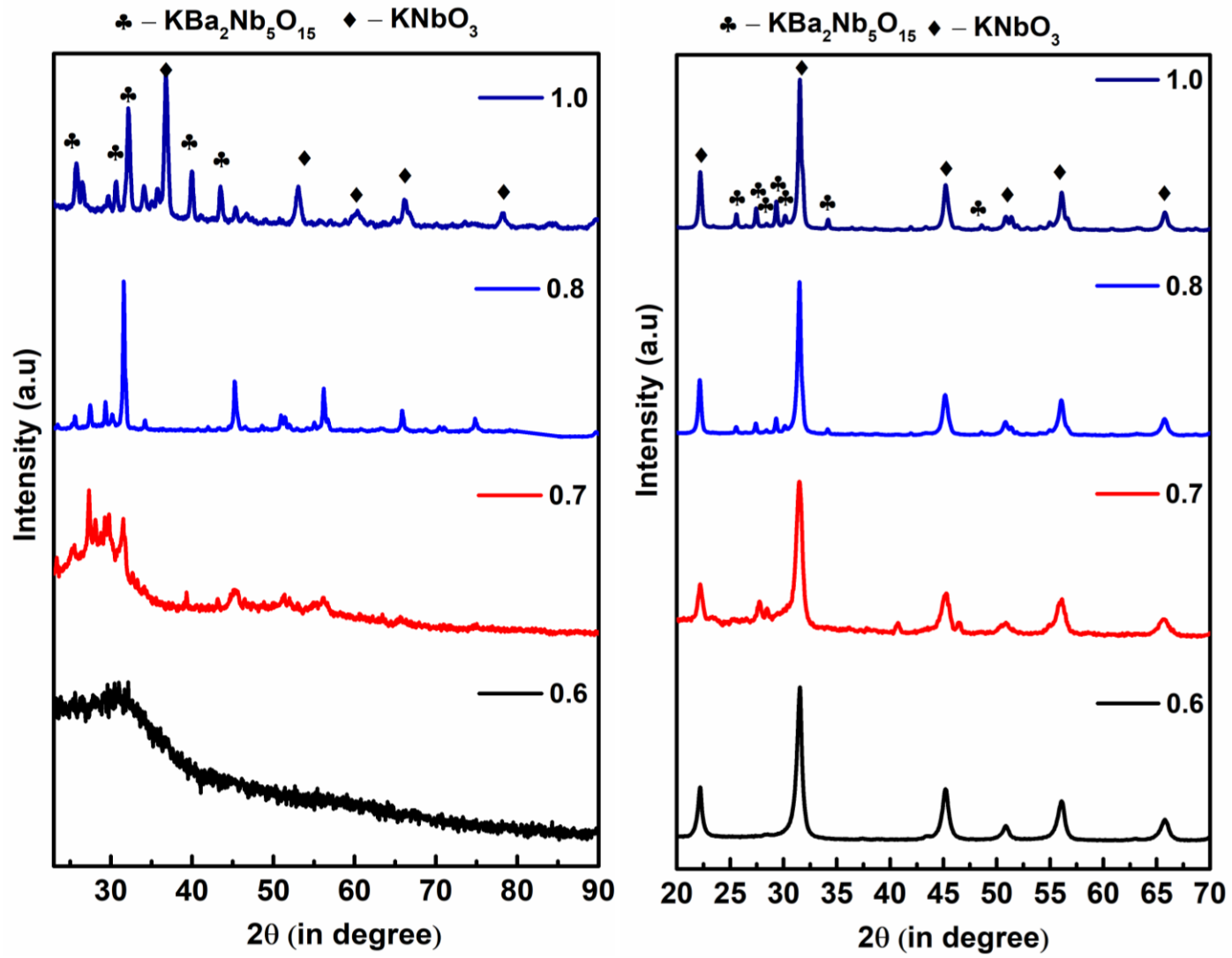

Fig 1 a) XRD of as fired powder after combustion with varying ϕ_e
b) XRD of calcined samples with varying ϕ_e

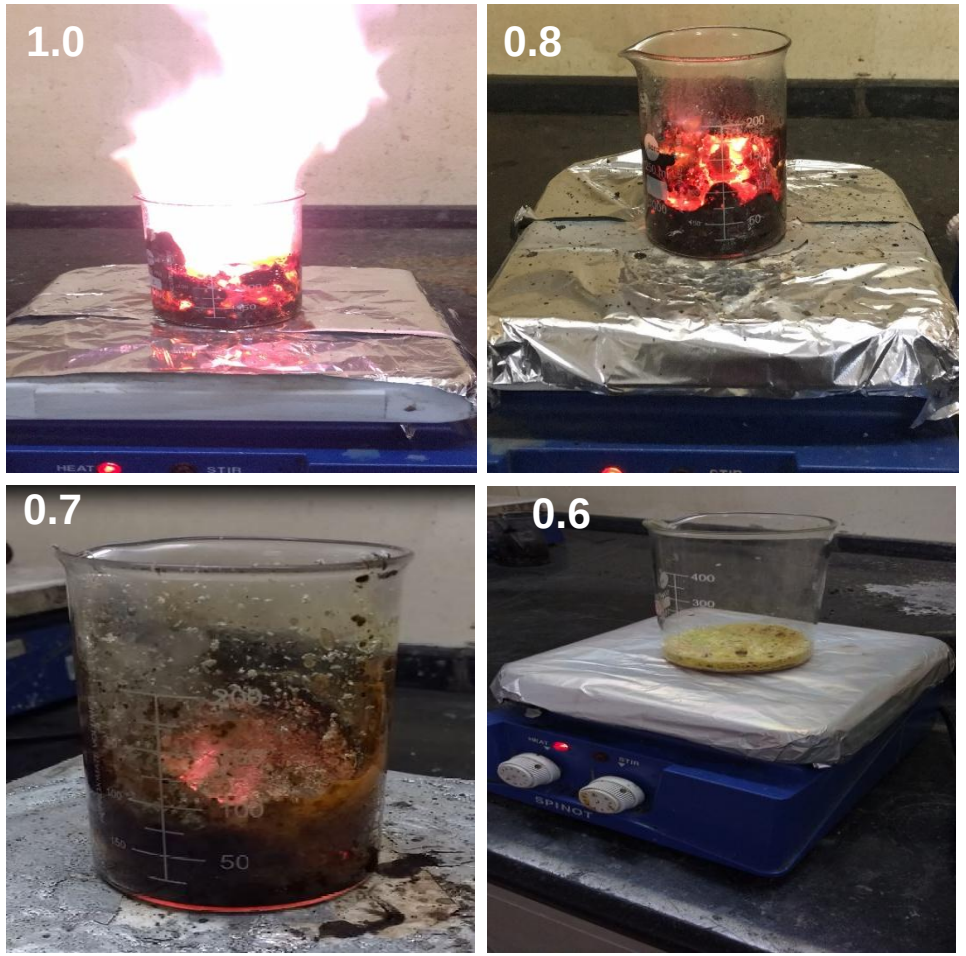

Fig 2 Combustion nature with varying ϕ_e

FTIR & XRD of gel samples at ϕ_e 0.6

- 2921 and 2853 cm^{-1} assigns to -CH2 symmetric and asymmetric stretching modes of citric acid.
- 1600 and 1380 cm^{-1} are due to stretching vibration modes of COO- bonds of citric acid.
- 1060 and 800 cm^{-1} are due to presence of carbon.
- 500 and 600 cm^{-1} O-Nb-O stretching vibrations of the corner-shared & corner sharing NbO6 octahedron

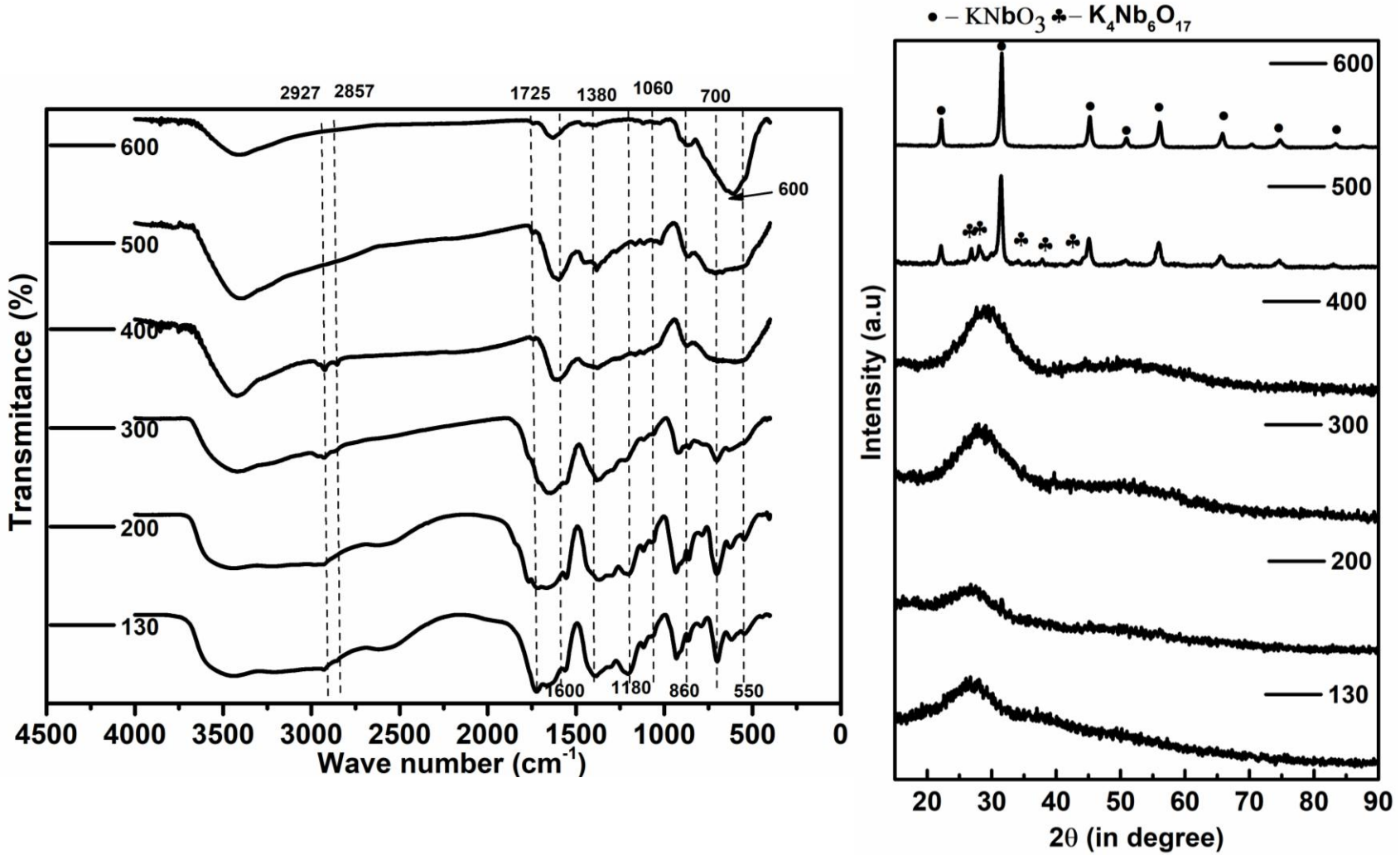

Fig 3 a, b) FTIR spectra & XRD of KBNNO 0.1 gel samples calcined at various temperatures

XRD & FESEM Micrographs

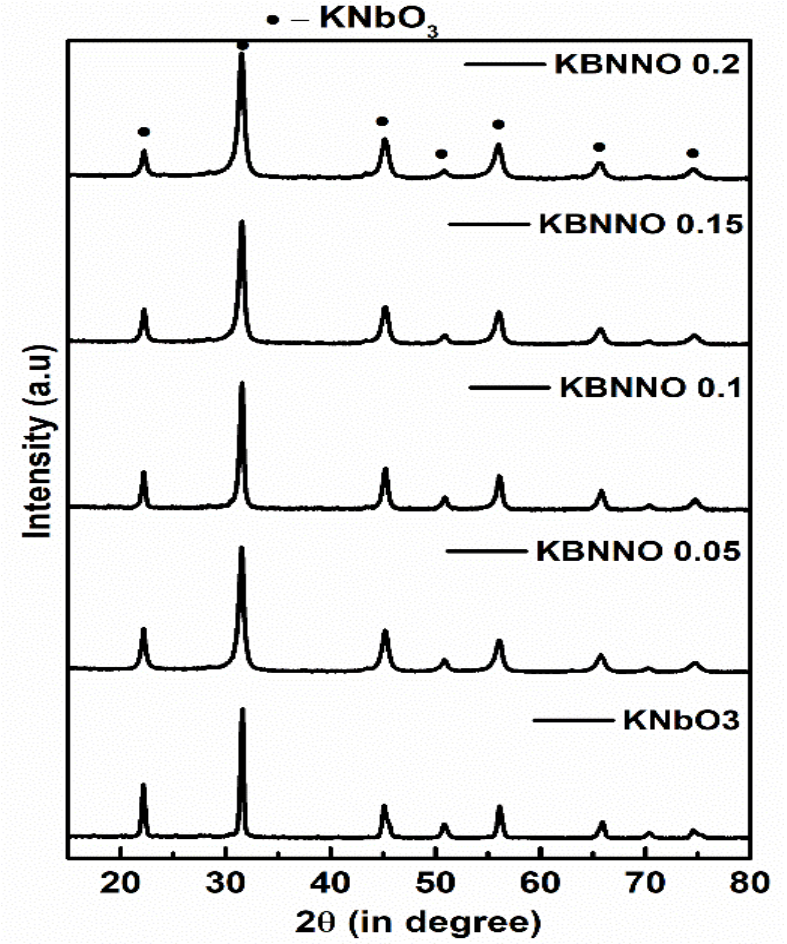

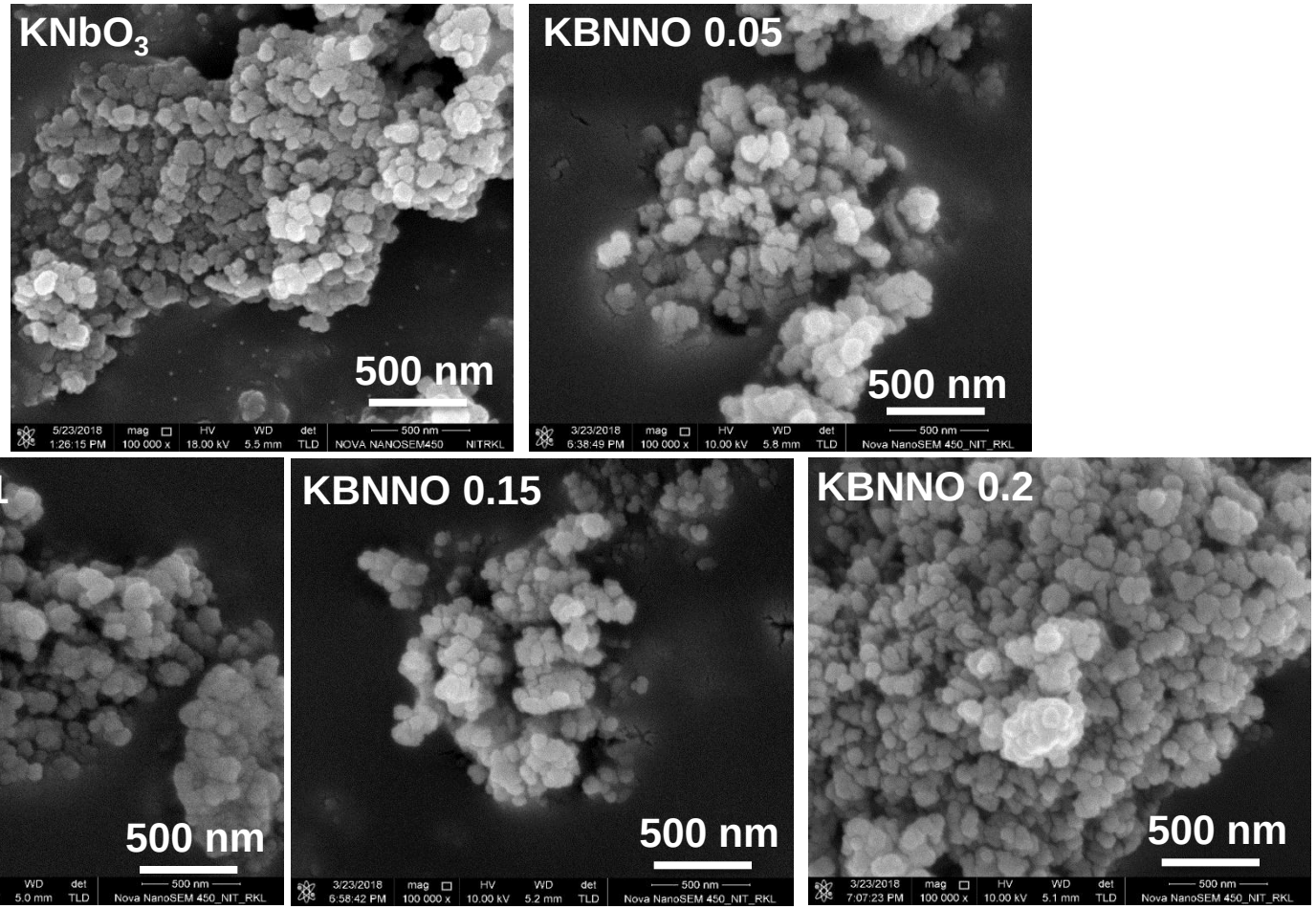

Fig 4: XRD and FESEM of $KNbO_3$ and Ba, Ni co-doped $KNbO_3$ samples calcined at 600°C

- FESEM micrographs shows nano particles and weakly agglomerated
- No clear information about particle size is observed

PL and UV-Vis spectroscopy

- PL spectroscopy shows peaks at 450, 490, 516 and 548 nm.
- Peaks in PL can be assigned to distorted NbO6 octahedron or oxygen vacancies.
- From UV-Vis Spectroscopy with increase in dopants concentration red shift is observed
- Broad absorption peaks are observed at 400-500 and 600-800 nm

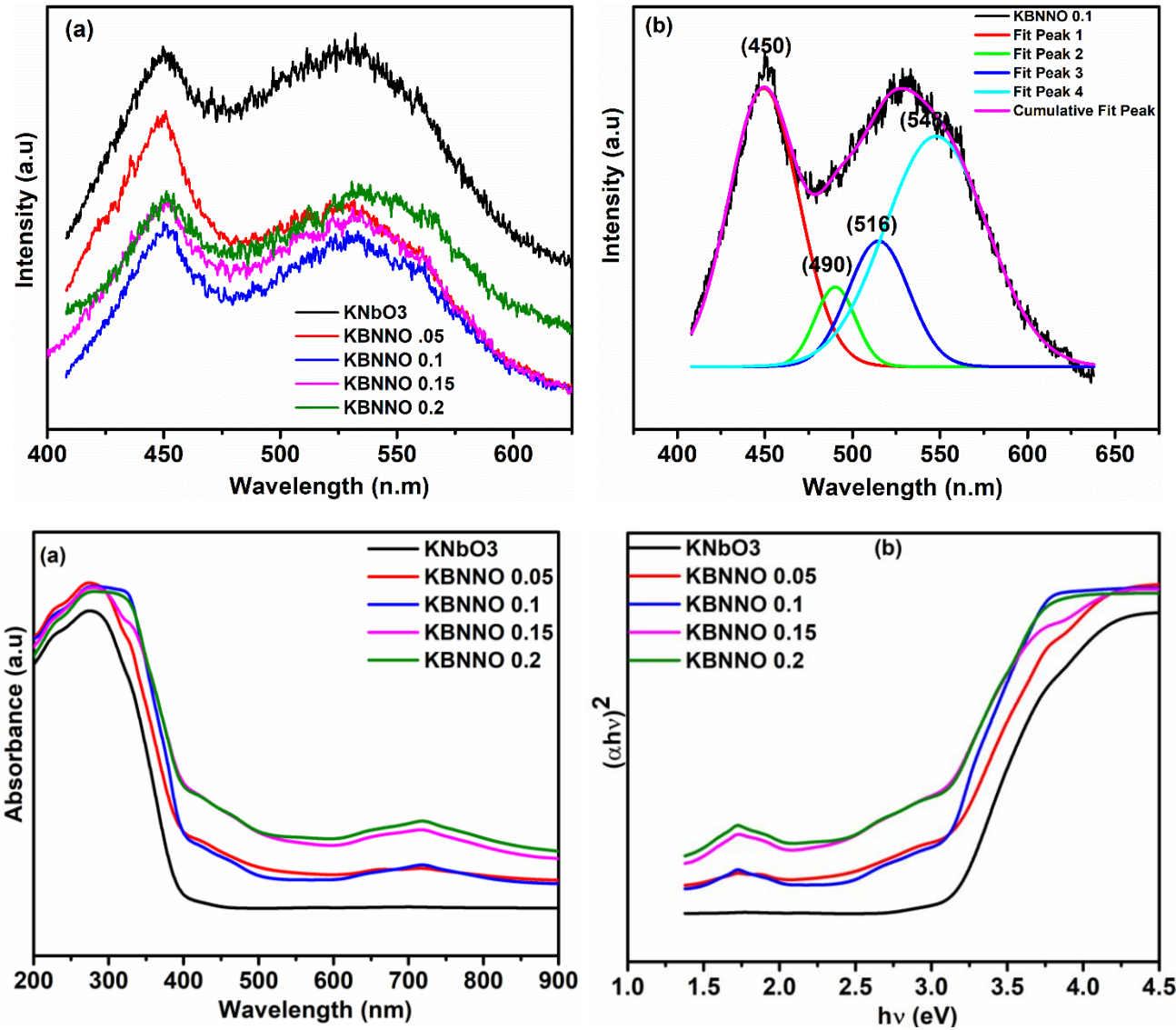

Fig 5: PL and UV spectra of $KNbO_3$ and Ba, Ni co-doped $KNbO_3$ samples calcined at 600°C

Photcatalysis

- Ba-Ni co-doped $KNbO_3$ samples show better photocatalytic activity when compared with pure $KNbO_3$ under UV light irradiation.
- $KNbO_3$ can degrade 53% of the dye whereas Ba, Ni co-doped $KNbO_3$ can degrade 79%, 93%, 87% and 84% of the dye after 60 mins of UV light irradiation for KBNNO0.05, KBNNO0.1, KBNNO0.15, KBNNO0.2, respectively.

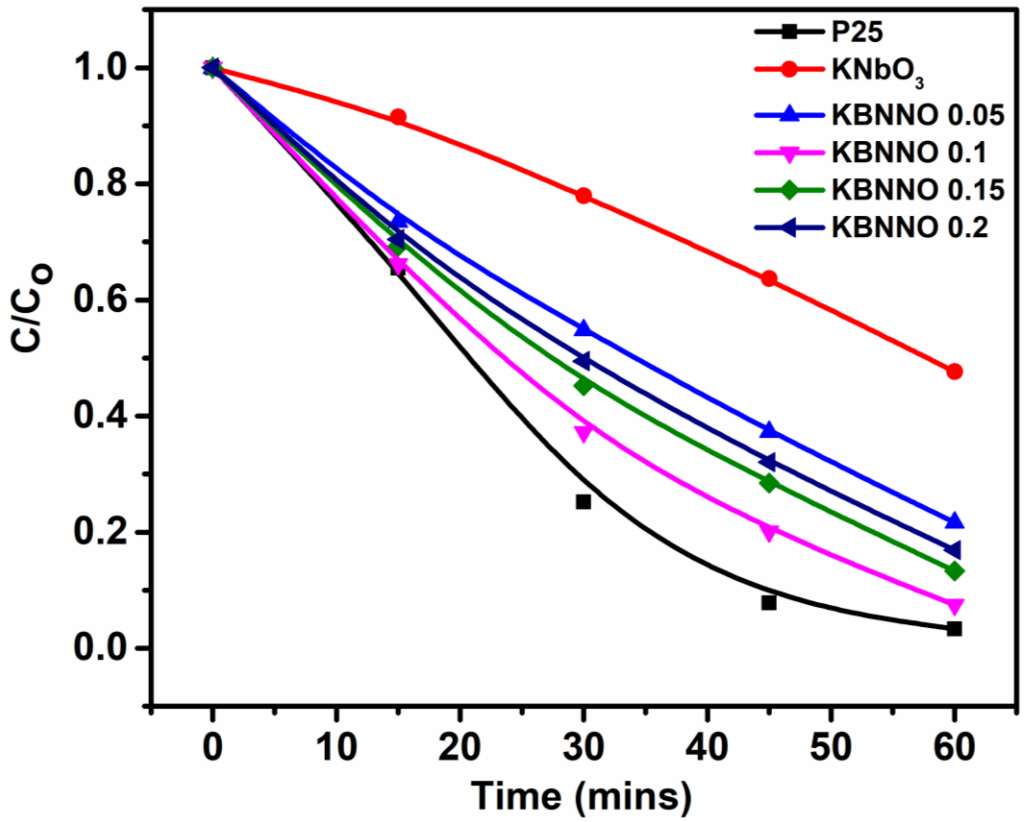

Fig 6: Change of concentration of RhB versus time under UV light irradiation

Conclusions

- Phase pure KBNNO nanopowder was synthesized by solution combustion method using citric acid as the fuel. The fuel-to-oxidizer ratio (Φe) (0.6–1.0) has significant effect on the combustion process and phase evolution.
- FTIR and XRD of the gel/powder samples shows that complete phase formation occurs at 600^{o}C.
- Raman spectroscopy shows that change in crystal structure from orthorhombic to cubic form for higher concentration of dopants.
- SAED patterns shows the high crystallinity of KBNNO 0.1 sample.
- PL spectroscopy indicates the lowering of electron-hole recombination rate in KBNNO0.1 compared to $KNbO_3$.
- UV-Visible spectroscopy shows that significant absorption in visible region.
- Enhanced photocatalytic activity of KBNNO 0.1 samples in comparison to $KNbO_3$, solid state derived KBNNO 0.1 and P25 in visible light.

Acknowledgement

Director, NIT Rourkela and

Board of Research on Nuclear Science


Thank You